Journal Name

ARTICLE

Photosensitised selective semi-oxidation of tetrahydroisoquinoline: A singlet oxygen path‡

Received 00th January 20xx,
Accepted 00th January 20xx

DOI: 10.1039/x0xx00000x

www.rsc.org/

Mahzad Yaghmaei,[a] Martin Villanueva,[a,b] Iris Martín-Garcia [a,c], Francisco Alonso[c], Xiaocong Zhang [a], Neeraj Joshi [a], Anabel E. Lanterna,[a,e] and Juan C. Scaiano*[a]

Selective semi-oxidation of tetrahydroisoquinoline (THIQ) leads to a valuable dihydroisoquinoline (DHIQ) derivative via singlet oxygen photooxidation process. Typical photosensitisers (i.e., Ru complexes) can activate the reaction even under heterogeneous conditions that facilitate catalyst separation and reusability. In contrast to DHIQ, THIQ acts as an efficient singlet oxygen quencher driving the reaction selectivity. The reaction can also be facilitated by semiconductor catalysts such as MoCo@GW, a glass wool-based catalyst that is easy to separate and reuse and compatible with flow photochemistry. Its role is to mediate the formation of isoquinoline (IQ) and thus an *in situ* generated singlet oxygen catalyst. Laser flash photolysis with NIR detection provides proof of the singlet oxygen mechanism proposed and rate constants for the key steps that mediate the oxidation.

Introduction

Reactions that involve partial hydrogenation or de-hydrogenation present selectivity challenges due to catalytic processes that tend to proceed to completion; for example, we recently reported on the reduction of alkynes, where it is easy to proceed completely to the alkane, but difficult to stop "half way" at the alkene.[1, 2] In the case of oxidations, a similar characteristic is common, for example the overoxidation of 1,2,3,4-tetrahydroisoquinoline (THIQ) to yield isoquinoline (IQ) is common, while stopping at the semi-oxidation product – dihydroquinoline (DHIQ) is challenging and requires highly selective catalysts. This is reflected in commercial pricing, where DHIQ is 70 times more expensive than THIQ and 200 times more expensive than IQ.[3] The possibility of carrying out these selective transformations with reusable catalysts and utilising molecular oxygen constitute a preferred sustainable pathway. Badu-Tawiah et al.[4] have recently reported on the photocatalytic aerobic dehydrogenation of tetrahydroquinolines (THQ) and THIQ derivatives. While they recognise THIQ oxidation is frequently incomplete, they attribute this unusual reactivity to the hyper-conjugation of the molecule and use N-substituted derivatives to achieve full oxidation. Contrasting reports suggest the formation of singlet oxygen under photocatalytic conditions can be either detrimental[5] or essential[6] when considering aerobic oxidation of N-substituted THIQ to their corresponding isoquinoline derivatives. In this work, we show singlet oxygen is essential for the dehydrogenation of THIQ and that the oxidation process is stalled until minimal concentrations of IQ are generated *in situ* during the reaction, driving selectivity towards the semi-oxidation product DHIQ.

Oxidation of THIQ with visible showed an induction delay before the reaction starts. Using different solvents with different oxygen solubility affected the reaction delay time, and experiments with deuterated methanols with various singlet oxygen lifetimes suggested the involvement of singlet oxygen in this reaction. Further experiments with laser flash photolysis were a confirmation on the main role of singlet oxygen in THIQ oxidation.

The mechanistic studies shown here test a recently introduced photocatalyst based glass wool as an inexpensive, widely available catalyst support that with adequate surface modification can provide physical or chemical affinity towards numerous catalytic materials.[7, 8] We use heterogeneous and homogeneous catalysts, a newly designed molybdenum disulfide-cobalt semi-conductor catalyst (MoCo@GW) and a modified $Ru(bpy)_3Cl_2$ (RuB@GW}, both supported on glass wool, and commercial $Ru(bpy)_3Cl_2$ were added to the reaction mixture. Remarkably, these catalysts allow for selective photooxidation to dihydroisoquinoline (DHIQ), avoiding common overoxidation to isoquinoline (IQ), under oxygen atmosphere, room temperature, and visible light irradiation.

[a] Department of Chemistry and Biomolecular Sciences and Centre for Advanced Materials Research (CAMaR), University of Ottawa, Ottawa, Ontario, Canada K1N 6N5
[b] Present address: Universidad Nacional de Córdoba, Facultad de Ciencias Químicas, Ciudad Universitaria, X5000HUA, Córdoba Argentina.
[c] Present address: Instituto de Síntesis Orgánica and Departamento de Química Orgánica, Facultad de Ciencias, Universidad de Alicante, Apdo. 99, 03080 Alicante (Spain)
[d] Present address: Department of Chemistry, McGill University, 801 Sherbrooke St W, Montreal, QC, Canada, H3A 0B8
[e] Present address: School of Chemistry, University of Nottingham, University Park, Nottingham,

Supplementary information includes details of catalyst preparation and characterization, XPS data and additional conversion/selectivity graphs.

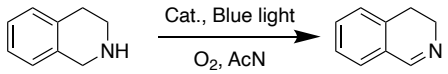

Scheme 1. Selective oxidation of THIQ to DHIQ catalysed by supported Ru@GW, MoCo@GW or soluble $Ru(bpy)_3Cl_2$. When no catalyst is added the reaction shows a prolongued induction period until catalyst is generated *in situ.*

The reaction was performed under blue light excitation (wavelength centred at ~450 nm) and an oxygen atmosphere. For catalytic experiments 50 mg of the heterogeneous catalyst were used. Kinetic studies show a long induction period for the reaction to start; for example, under an irradiance of ≤6 Wcm^{-2}, it takes as long as 90 minutes to achieve the first 10% conversion, followed by a dramatic acceleration of the partial oxidation to DHIQ (*vide infra*). Given the high value-added for DHIQ we decided to undertake a mechanistic study of this semi-oxidation step and the parameters that control the rate, initial delay, and selectivity of the process. Our studies show that MoCo@GW can perform single electron transfer (SET) reactions (even if inefficiently) that can get the oxidation started and eventually produce enough IQ that can accelerate the reaction through efficient singlet oxygen mechanisms. While alternative direct photosensitization to generate singlet oxygen (e.g., with soluble $Ru(bpy)_3Cl_2$) allows a delay-free oxidation process, the use of MoCo@GW has the advantage of being readily removable from the reaction media and also potentially compatible with flow photocatalysis.

We combine catalyst characterization and bench studies with laser flash photolysis which under a variety of conditions – including near infrared detection – lead to compelling kinetic information showing the role of singlet oxygen in the advanced stages of the reaction and lead to information enabling the reduction or elimination of the initial reaction delay.

Experimental

See ESI for additional information on experimental conditions, sources of materials and spectroscopic and analytical conditions.

Conditions of irradiation

The standard conditions for reaction involved 67 mg of THIQ (0.125 M) in 4 mL of acetonitrile, irradiated with ≤ 6 Wcm^{-2} of LED light centered at ~450 nm (LEDi, Luzchem LED Illuminator with FWHM 23 nm) under O_2 atmosphere with air cooled samples maintained at ~23 °C. A detailed spectroscopic analysis of this light source reveals that it contains 0.02% of light below 400 nm.

Laser flash photolysis and NIR detection

The laser flash photolysis experiments were performed using a Surelite Nd-YAG laser 355 nm (~10-20 mJ/pulse) in a customized LFP-111 laser-flash photolysis (LFP) system (Luzchem Inc., Ottawa, Canada) and 1×1 cm^2 or 0.7 x 0.7 cm^2 LFP cuvettes from-Luzchem. Samples had an absorbance of ~0.3 at the laser wavelength.

Time resolved singlet oxygen luminescence measurements were conducted using the same laser system as above and were detected at right angles using a Hamamatsu photomultiplier tube sensitive in the near-IR. The signal was captured and digitized using a Tektronix 2440 transient digitizer part of the customized Luzchem laser flash photolysis system. Singlet oxygen measurements were made at 1270 nm with samples having absorbances at 355 nm in the range of 0.1 - 0.4.

Synthesis and characterization of MoCo@GW catalyst

Initial requirements for the active species attachment have implied the activation of the non-silanized glass wool with a source of amino- groups given by (3-aminopropyl)-triethoxysilane (APTES) treatment. The catalyst was then synthesized by treating glass wool with 3.5 %wt of Mo and a 5.4 %wt Co load. Metallic species were grafted (chemisorption) to the APTES@GW fibers using a photochemical method. Briefly, proper amounts of Mo and Co precursors were mixed with the photoinitiator Irgacure 907 (I-907) in a flask using acetonitrile as reaction solvent. This initiator can undergo Norrish type I cleavage upon UVA excitation generating radical species that can reduce the metal cations, also improving the attachment of cobalt oxide (CoO_x) nanoparticles to the Mo layered matrix. Mo and Co proportions were determined by ICP-OES analysis (Table S1). Additionally, through comparisons with the only-Mo (Mo@GW) and only Co (Co@GW) control catalysts, we found that mix of both Mo and Co (MoCo@GW) is more efficient than their single metal catalysts same as reported by others.[9] Scanning electron microscopy (SEM) allowed us to observe the particles and a similar distribution of Mo and Co determined by EDS analyses on fibers; images of the complete fibers show that cobalt centers are located in the same area as the molybdenum structures (Figure S1). By using x-ray photoelectron microscopy (XPS) characterization the oxidation states of Mo 3d and Co 2p were detected. Mix of Mo^{4+}, Mo^{6+} and Co^{2+} observed for MoCo@GW (Figure S2).

Results and Discussion

Experiments without catalyst

The selective oxidation of THIQ was studied under different conditions. In the absence of any catalyst, THIQ solutions in acetonitrile are stable under dark conditions. The system also shows minimal changes for at least two hours under visible light (λ = 450 nm) irradiation. Prolonged irradiation leads to small conversions to DHIQ (10 % after 370 min), after which the reaction accelerates and reaches a conversion rate of 0.51% per minute near the inflexion point, see Figure 1. The reaction reaches 90% selectivity towards DHIQ [i.e.,100 x DHIQ/(DHIQ + IQ)] at 50% conversion and remains at 82% selectivity at 98.5% conversion. The drastic acceleration of the reaction shown in Figure 1 suggests a slow *in situ* formation of efficient catalytic species within the reaction, which were further analysed by LFP (see below). Notably, the reaction performs poorly in air and does not proceed under an inert atmosphere (Figure S3).

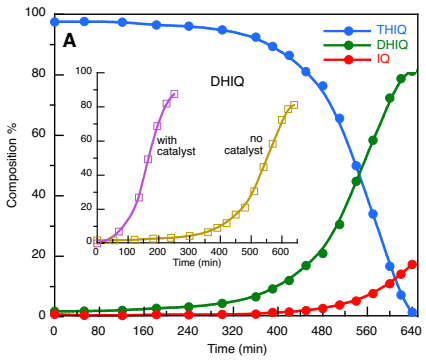

Figure 1: Evolution of the semi-oxidation of THIQ (0.125 M) in AcN under Blue LEDi (~450 nm) irradiation and O_2 atmosphere in the absence of catalyst and (inset) a comparison of DHIQ formation when the catalyst is MoCo@GW.

Close analysis of the reaction evolution experiments indicate that the maximum conversion rate, as measured at the inflexion point in the THIQ curve, coincided with the presence of small (≤2%) formation of IQ. To better understand the role of IQ in the selective oxidation of THIQ, we performed a series of experiments introducing small quantities of IQ at different reaction times (Figure S4). Addition of 4 %mol equivalents of IQ at the start of the reaction reduced the initial delay (to 10% conversion) from 370 to 210 minutes. Effect of addition of 4 %mol DIQ was less than IQ addition. Further, adding 0.5 mL of a completed reaction to a 4 mL fresh sample reduced the delay to 35 minutes, doubling the conversion rate (figure S4).

Another way to test the effect of pre-irradiation is to add THIQ when the reaction is almost completed as illustrated in Figure 2, where THIQ was added after 600 minutes. Notice that no delay is detectable after the addition of THIQ, suggesting that the solution was "ready" to proceed with the photocatalytic process.

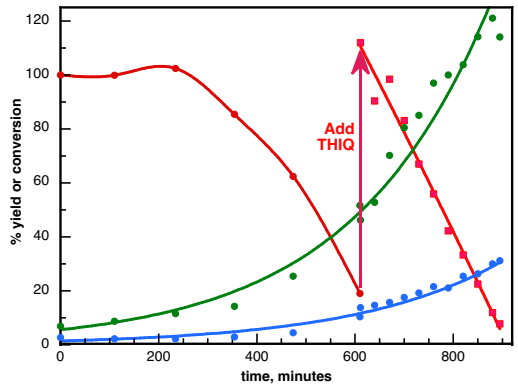

Figure 2: THIQ oxidation reaction evolution over time under conditions described in Figure 1, followed by addition of THIQ (to reach 0.125 M) at 611 minutes. Notice that after addition of THIQ, DHIQ and IQ follow a smooth growth curve, while consumption of THIQ occurs without delay. Selectivity was 79% after 900 minutes.

Solvent effects

The reaction conditions shown in Figure 1 were used to test different solvents, namely acetonitrile, hexane (Hx), and methanol (MeOH). The solvents were selected based on their different oxygen solubility (Hx > Acetonitrile > MeOH) and polarity (dielectric constant: Hx < Acetonitrile ~ MeOH) or ET(30) (Hx > MeOH > Acetonitrile).[10] Figure 3 shows that methanol is the least efficient solvent because of the long initial delay and the low rate of THIQ consumption, effectively almost 5 times slower than in acetonitrile. This led us to suspect that singlet oxygen could be mediating the late stages (post initial delay) of the oxidation of THIQ. To test this possibility, we substituted methanol for CD_3OD, as deuteration is known to enhance dramatically the lifetime of singlet oxygen.[11] As illustrated in Figure 3, CD_3OD causes a significant acceleration of the overall process, as expected for singlet oxygen reactions, reflecting that THIQ reactions will be favoured if the lifetime of singlet oxygen is enhanced.[11] The effect for CH_3OD (not shown) is minor, reflecting a minor $^1O_2$ lifetime enhancement.

As a further test of the singlet oxygen hypothesis, we added NaN_3 to the system, as N_3^- is a well-known singlet oxygen scavenger.[12] This led to a small slow-down of the reaction (figure S7). The usual extensive effect of azide is probably attenuated by the fact that THIQ is itself an excellent singlet oxygen scavenger. On the other hand adding $Ru(bpy)_3Cl_2$ as a singlet oxygen sensitizer to the THIQ showed a reaction without any delay Figure S5.

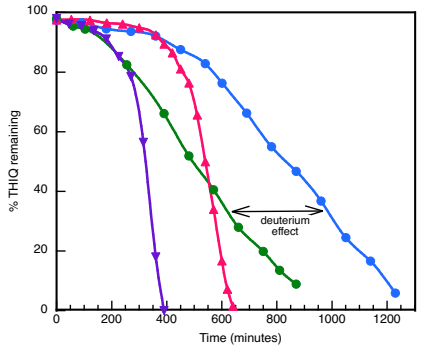

Figure 3: Consumption of THIQ as a function of time in various solvents: Purple triangles = hexane, pink triangles = acetonitrile, blue circles = methanol and green circles = methanol-d_4. Note that methanol-d_4 accelerates the reaction by ~ 360 minutes.

Mechanistic studies

As the next step we decided to examine the possible role of singlet oxygen making its generation independent of the THIQ system. For this purpose, we used $Ru(bpy)_3Cl_2$ as a commercially available sensitizer, using 355 nm laser pulses for excitation and monitoring the emission from singlet oxygen in acetonitrile at 1270 nm. The lifetime in the absence of quencher was ~80 μs (τ_0), which is consistent with literature reports for singlet oxygen in acetonitrile.[13, 14] The lifetimes were reduced in the presence of THIQ, as illustrated in the inset in Figure 4. A plot of the rate constant for decay (k_d) as a function of the THIQ concentration (equation 1) leads to a quenching rate constant of 2.63 x 10^7 $M^{-1}s^{-1}$.

$$k_d = \tau^{-1} = \tau_0^{-1} + k_q[THIQ] \qquad (1)$$

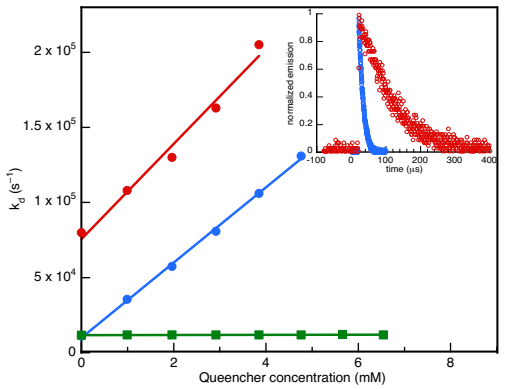

Figure 4: Quenching plots for singlet oxygen in acetonitrile. Blue and red points for THIQ with $Ru(bpy)_3Cl_2$ and IQ as sensitizers, respectively. Green points are for DHIQ as quencher, with $Ru(bpy)_3Cl_2$ as sensitizer. No significant quenching is observed for DHIQ. Inset: decay traces for singlet oxygen emission (monitored at 1270 nm) in the absence (red) and presence of 0.0029 M THIQ (blue). For long lifetimes (red data) it is necessary to attenuate the signal to obtain more reliable lifetimes.

As discussed before, the presence of IQ can accelerate the oxidation of THIQ (Figure 2). To understand this apparent *in situ* catalytic effect, we explored the potential formation of singlet oxygen using IQ as sensitiser. The experiment needed to be performed at a rather high IQ concentration that led to a reduction of singlet oxygen lifetimes; however, the identification of the emitter was unequivocal and the rate constant for THIQ quenching was the same as in $Ru(bpy)_3Cl_2$ experiments. What is more, similar $Ru(bpy)_3Cl_2$ experiments with DHIQ as a quencher revealed that singlet oxygen quenching by DHIQ is at least 1000 times slower than by THIQ (Figure 4), an observation that is key to the high discrimination towards selective oxidation observed in our work.

Heterogeneous Catalysts

We tried several catalysts to test the oxidation dymanics without affecting the selectivity. While the experiments above show that singlet oxygen generators can greatly enhance the kinetics of THIQ to DHIQ conversion with minimal loss of selectivity, it would be desirable to avoid soluble catalysts that add steps to the post-reaction separation and purification processes. For this purpose, we tested if the ruthenium catalysis could be performed by a heterogeneous catalyst also capable of generation of singlet oxygen but being amenable for easy removal after use. We have previously developed glass-grafted ruthenium catalysts, among them the $[Ru(bpy)_2dppa](PF_6)_2$ loaded onto glass wool (RuB@GW).[8] As shown in Figure 5A, irradiation of RuB@GW confirmed the conversion of THIQ to DHIQ without an extended initial delay, in reasonable time (that could be adjusted with light intensity) and with excellent selectivity.

The same reaction conditions were assayed in the presence of 50 mg of MoCo@GW and the initial delay was shortened to ~80 min for 10% conversion and the rate at the inflexion point increased to 0.82% per minute. At 90% conversion (225 min) the selectivity was still 90%, Figure 5B. As a control experiment for using a bimetallic catalyst, we prepared Mo@GW, Co@GW, and APTES@GW and ran the experiment with the same conditions (Figure S6). The results confirmed the synergistic effect between Mo and Co in improving catalytic role in oxidation reaction.[15, 16]

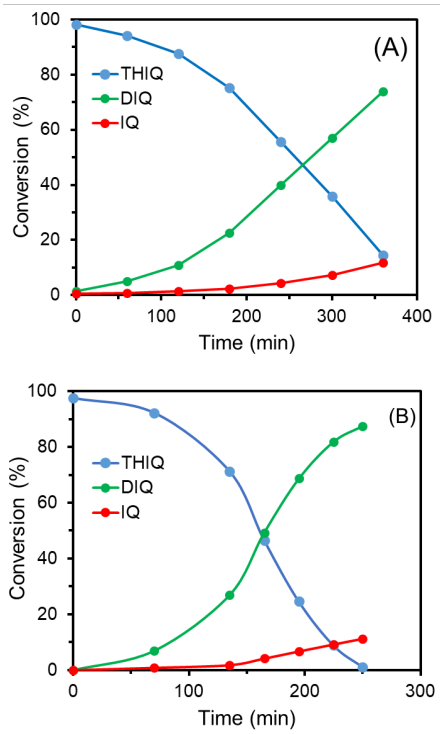

Figure 5: THIQ oxidation reaction evolution over time under visible light irradiation in the presence of (A) RuB@GW and (B) MoCo@GW. Conditions: THIQ (0.125 M), acetonitrile, O_2 atmosphere, λ= 450 nm (≤ 6 W cm^{-2}). THIQ in blue, DHIQ in green and IQ in red.

Mechanistic analysis

There are two aspects to the oxidative generation of DHIQ from THIQ. One is straightforward and is the singlet oxygen mediated oxidation. With a quenching rate constant of 2.6 x 10^7 $M^{-1}s^{-1}$ THIQ is a favoured target for singlet oxygen reaction. Further, the fact that DHIQ is a poor singlet oxygen target, with its reaction at least 1000 times slower than for THIQ is the cause of the high selectivity that helps the oxidation to stop "halfway" rather than proceed to IQ.

The second aspect is the initiation of the process in the absence of added singlet oxygen sensitizers. Since all indications are that in all cases singlet oxygen is the dominant reaction mechanism, in the cases with no sensitiser added, or with MoCo@GW as a pre-catalyst we require a route for the *in-situ* generation of a singlet oxygen sensitizer, with the simplest explanation (and confirmed by chromatographic analysis) is the formation of IQ. For the no-catalyst system, with nearly 6 hours delay under strong irradiation. It is hard to identify a source, although it is hardly surprising that some oxidation takes place, noting also that once some IQ is generated it can support further oxidation. Further, as much as 0.7% IQ may be present in the initial reaction mix.

The presence of MoCo@GW greatly reduces the delay. We propose that the formation of IQ in this case is also mediated by DHIQ which is an excellent target for HOO• radicals (given the presence of benzylic hydrogens),[17] with DHIQ formed by the mechanisms of Scheme 2.

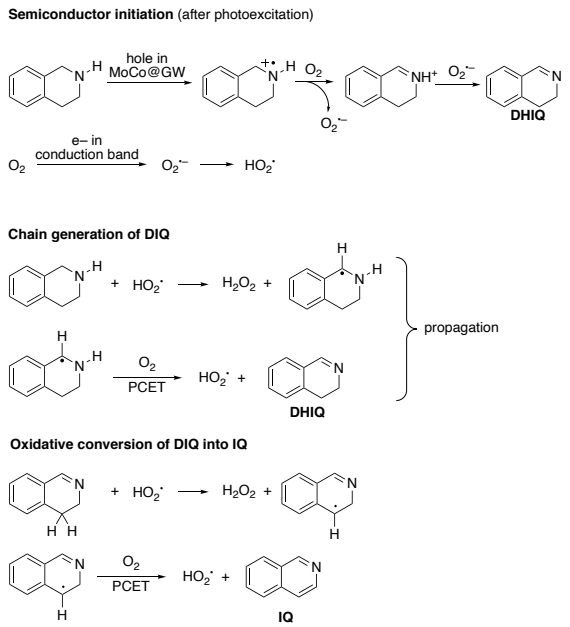

Scheme 2: Semiconductor based mechanisms for the formation of DHIQ, a precursor for IQ under semiconductor mediated oxidation.

The complexity of Scheme 2 is entirely related to the need to add or generate *in situ* a good singlet oxygen sensitizer; once this has been achieved the singlet oxygen oxidation takes over and ensures the excellent selectivity towards DHIQ. In fact, the mechanism of Scheme 2, which enables the initial formation of IQ, would not be anticipated to provide the selectivity towards DHIQ that is at the centre of this report.

Conclusions

For the series THIQ. DHIQ and IQ, the most valuable one is DHIQ, largely reflecting that both for catalytic oxidations and reductions, stopping "halfway" is difficult. Catalysts that utilize molecular oxygen are highly desirable as they enable sustainable pathways, more so if they are heterogeneous catalysts, easy to recover and suitable or adaptable flow chemistry.

In the case of THIQ the dramatic difference in reactivity towards singlet oxygen between THIQ and DHIQ (≤1000) enables exceptional selectivity and the ability to stop "halfway" in the oxidative process.

Conflicts of interest

There are no conflicts to declare.

Acknowledgements

This work was supported by the Natural Sciences and Engineering Research Council of Canada, the Canada Foundation for Innovation, and the Canada Research Chairs Program. We also thank the Spanish Ministerio de Ciencia e Innovación (MCIN; grant no. CTQ2017-88171-P) and the Generalitat Valenciana (GV; grant no. AICO/2017/007) for financial support. Thanks are due to Dr. R. I. Teixeira for the synthesis of RuB@GW during his 2019 visit to Ottawa.

Notes and references

‡ Dedicated to Dr. Silvia Braslavsky as her amazing journey through science brings her to a memorable landmark.

1. B. Wang, K. Duke, J. C. Scaiano and A. E. Lanterna, Cobalt-Molybdenum co-Catalyst for Heterogeneous Photocatalytic H-mediated Transformations, J. Catal., 2019, 379, 33-38.
2. F. Alonso, I. Osante and M. Yus, Highly Stereoselective Semihydrogenation of Alkynes Promoted by Nickel(0) Nanoparticles, Adv. Synth. Catal., 2006, 348, 305-308.
3. Sigma Aldrich website (https://www.sigmaaldrich.com/canada-english.html) consulted on 13-March-2021.
4. S. Jayaraj and A. K. Badu-Tawiah, N-Substituted Auxiliaries for Aerobic Dehydrogenation of Tetrahydro-isoquinoline: A Theory-Guided Photo-Catalytic Design, Sci. Rep., 2019, 9, 11280.
5. K. C. C. Aganda, B. Hong and A. Lee, Aerobic α-Oxidation of N-Substituted Tetrahydroisoquinolines to Dihydroisoquinolones via Organo-photocatalysis, Adv. Synth. Catal., 2019, 361, 1124-1129.
6. J. L. Clark, J. E. Hill, I. D. Rettig, J. J. Beres, R. Ziniuk, T. Y. Ohulchanskyy, T. M. McCormick and M. R. Detty, Importance of Singlet Oxygen in Photocatalytic Reactions of 2-Aryl-1,2,3,4-tetrahydroisoquinolines Using Chalcogenorosamine Photocatalysts, Organometallics, 2019, 38, 2431-2442.
7. A. Elhage, B. Wang, N. Marina, M. L. Marin, M. Cruz, A. E. Lanterna and J. C. Scaiano, Glass wool: a novel support for heterogeneous catalysis, Chem. Sci., 2018, 9, 6844-6852.
8. R. I. Teixeira, N. C. de Lucas, S. J. Garden, A. E. Lanterna and J. C. Scaiano, Glass wool supported ruthenium complexes: versatile, recyclable heterogeneous photoredox catalysts, Cat. Sci. Tech., 2020, 10, 1273-1280.
9. W. Zhong, M. Liu, J. Dai, J. Yang, L. Mao and D. Yin, Synergistic hollow CoMo oxide dual catalysis for tandem oxygen transfer: Preferred aerobic epoxidation of cyclohexene to 1,2-epoxycyclohexane, Appl. Catal. B: Environ., 2018, 225, 180-196.
10. M. Quaranta, M. Murkovic and I. Klimant, A new method to measure oxygen solubility in organic solvents through optical oxygen sensing, Analyst, 2013, 138, 6243-6245.
11. N. J. Turro, V. Ramamurthy and J. C. Scaiano, Modern Molecular Photochemistry of Organic Molecules, University Science Publishers, New York, N.Y., 2010.
12. J. R. Harbour and S. L. Issler, Involvement of the azide radical in the quenching of singlet oxygen by azide anion in water, J. Am. Chem. Soc., 1982, 104, 903-905.
13. F. Wilkinson and J. G. Brummer, Rate Constants for the Decay and Reactions of the Lowest Electronically Excited State of Molecular Oxygen in Solution, J. Phys. Chem. Ref. Data, 1981, 10, 809-999.
14. F. Wilkinson, W. P. Helman and A. B. Ross, Rate constants for the decay and reactions of the lowest electronically excited singlet state of molecular oxygen in solution. An expanded and revised compilation, J. Phys. Chem. Ref. Data, 1995, 24, 663-945.

15. L. Kaluža, D. Gulková, Z. Vít and M. Zdražil, Effect of support type on the magnitude of synergism and promotion in CoMo sulphide hydrodesulphurisation catalyst, Appl. Catal. A-gen., 2007, 324, 30-35.
16. J. Ji, X. Duan, G. Qian, X. Zhou, G. Tong and W. Yuan, Towards an efficient CoMo/γ-Al2O3 catalyst using metal amine metallate as an active phase precursor: Enhanced hydrogen production by ammonia decomposition, Int. J. Hydrogen Ener., 2014, 39, 12490-12498.
17. J. Small, R.D., J. C. Scaiano and L. K. Patterson, Radical Processes in Lipids. A Laser Photolysis Study of tert-Butoxy Radical Reactivity Toward Fatty Acids, Photochem. Photobiol., 1978, 29, 49.

Journal Name

ARTICLE

Table of contents graphic

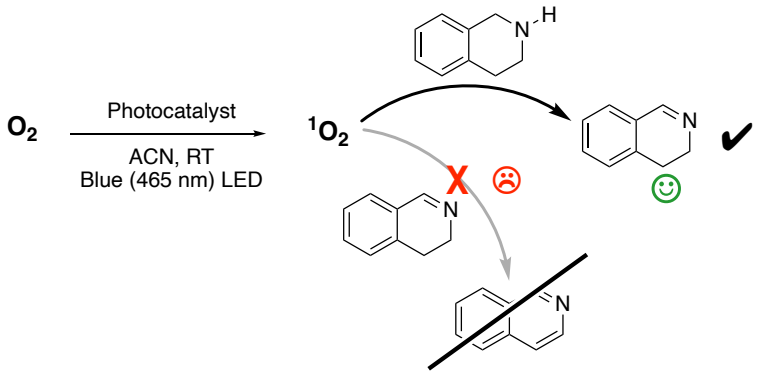

Graphical Abstract

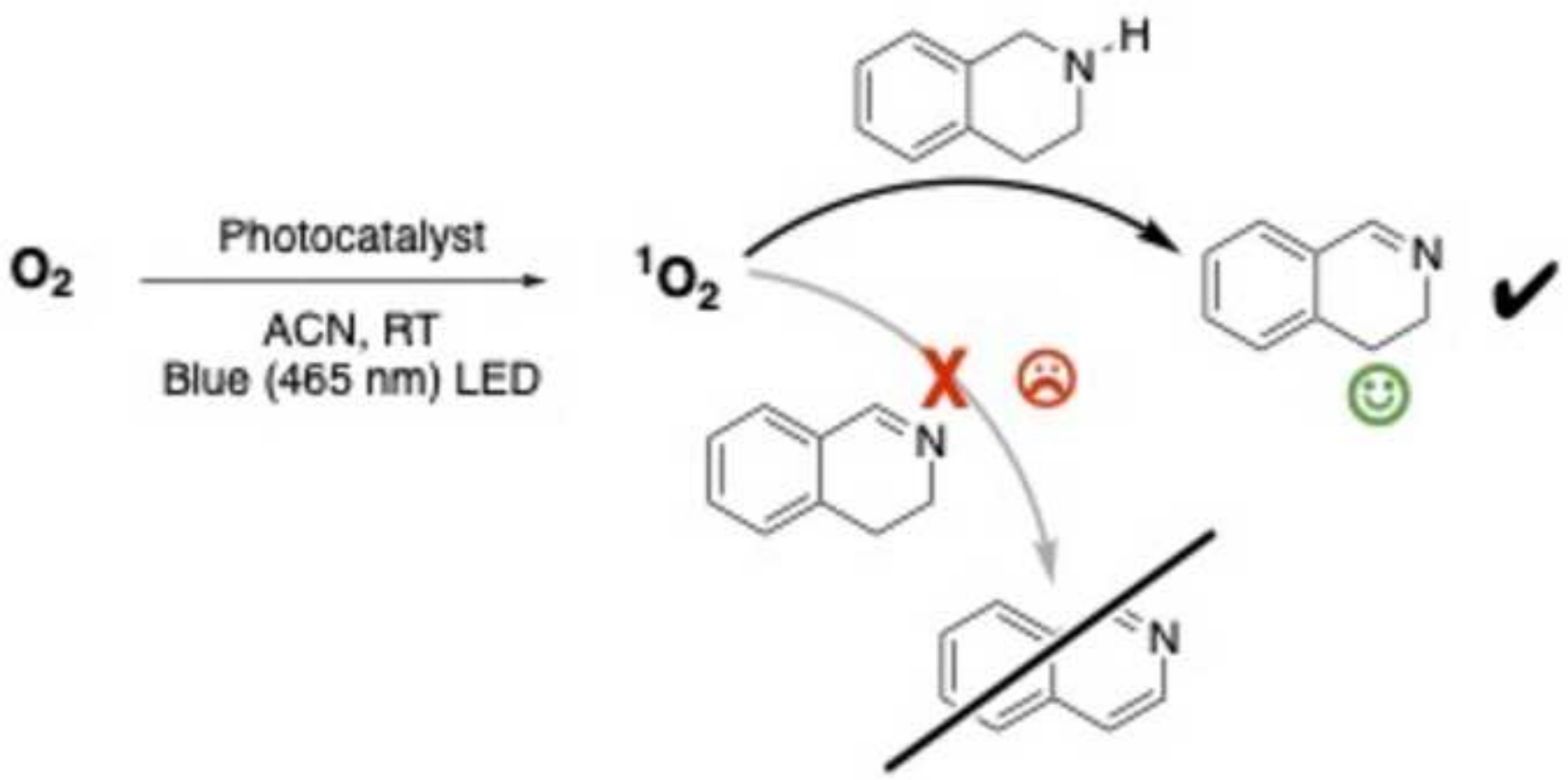

Photosensitised selective semi-oxidation of tetrahydroisoquinoline: A singlet oxygen path

Mahzad Yaghmaei, Martin Villanueva, Iris Martín-García, Francisco Alonso, Xiaocong Zhang, Anabel E. Lanterna, and Juan C. Scaiano*

Contents

Materials and instruments

Most of the compounds for doing experiments such as 1,2,3,4-tetrahydroisoquinoline, 3,4-dihydroisoquinoline, isoquinoline, cobalt(II) chloride hexahydrate and 3-aminopropyl)triethoxysilane, methanol-d4 were purchased from from Sigma Aldrich. Ammonium tetrathiomolybdate, 99.95% from Alfa Aesar and solvents were from Fisher chemical. UVA lamp 8W (LZC-UVA), blue LEDi 450 nm (LEDi-HBL) and Expo panel (EXPO-01) were from Luzchem Research, Inc.

The oxidation states of metals on glass wool were characterized by X-ray Photoelectron spectroscopy. XPS was performed on a Kratos analytical model Axis Ultra DLD, using monochromatic aluminum Ka X-rays at 140 W. XPS data were analyzed using CasaXPS software, Version 2.1.01. ICP experiments were performed using an Agilent Vista Pro ICP Emission Spectrometer and Scanning electron microscopy (SEM) and Energy dispersive X-ray spectroscopy (EDX) were performed in JEOL JSM-1600 SE microscope. All results analysed by GC-MS analyses from Agilent 6890-N Gas Chromatograph with an Agilent 5973 mass selective detector.

Catalyst preparation

Glass wool pre-treatment

A mass of 1 g of non-treated glass wool were placed in a round bottom flask and immersed in a 250 mL solution of 1% concentration of APTES in toluene. The mixture was refluxed overnight at 110°C to allow monolayer coverage. After that, a cooling down to room temperature of the mixture was allowed under constant stirring during 6 additional hours. Filtering process was done by washing the mixture with toluene (3x100 mL) and acetone (3x100 mL) then dried in the oven at 100°C overnight prior to metal decoration.[1]

Synthesis of MoCo@GW

Molybdenum and Cobalt supported on GW was prepared by photodeposition of $CoCl_2$ and $(NH_4)_4MoS_4$ onto the APTES treated GW. In brief, 9.6 mg of $(NH_4)_4MoS_4$ (3.5 wt% Mo), 21.8 mg of $CoCl_2.H_2O$ (5.4 wt% Co), and 18.4 mg of I-907 (photo-initiator) suspended in 10 mL of acetonitrile (AcN). The mixture was sonicated for 10 minutes, then added to 100 mg APTES@GW in glass vial then purged with Argon for 10 minutes. The sealed glass vial was irradiated with a Luzchem Expo panel fitted with 5 UVA bulbs (8W each) for 5 h and rotated on a hot-dog cooker for homogeneous mixing. The dark grey fibers obtained were filtered and washed with AcN to remove unreacted species and left to dry in the oven overnight. The resulting grey fibers were characterized by SEM, EDS, ICP, and XPS.

Similar procedures were followed for the synthesis of Mo@GW and Co@GW, using the corresponding metal precursor.

Synthesis of Mn@GW

MnO_2 supported on GW was prepared by reducing reaction of permanganate. 10 mg of $KMnO_4$ were dissolved in 10 mL of milli-Q water. 300 mg of APTES@GW were soaked in 10 mL of ethanol in a pyrex petri dish and the $KMnO_4$ solution was added. The mixture was kept in the dark and at room temperature for 3 h, then washed with ethanol and water to remove non bonded residual of MnO_2.

Synthesis of Ru@GW

The synthesis of this material has been described in the literature.[2]

Catalyst characterization

The catalysts were characterized by Inductively Coupled Plasma Optical Emission Spectroscopy (ICP-OES), Scanning Electron Microscopy (SEM), and X-ray Photoelectron spectroscopy (XPS).

ICP-OES analysis

Metal loading on freshly prepared MoCo@GW, Mo@GW, Co@GW, Mn@GW, and Ru@GW catalysts was determined by ICP-OES. Sample replicates of 20 mg of catalysts were accurately weighed, digested with aqua regia, and then diluted. The samples were measured and quantified by using the emission line of the corresponding elements (284.824 nm (Mo), 238.892 nm (Co), 267.876 nm (Ru), and 257.610 nm (Mn)). Table S1 shows the average results of ICP-OES for these samples.

Table S1. Metal loading determined by ICP-OES analysis

Catalyst	**M (wt%)**
MoCo@GW	0.146 (Mo)
	0.260 (Co)
Mo@GW	0.120
Co@GW	0.486
RuB@GW	0.002
Mn@GW	0.300

SEM analysis

Scanning electron microscopy analysis of the fresh and used MoCo@GW and Mn@GW were performed. SEM imaging and EDX analyses (

Figure S*1*) show that the surface of the glass fibre is covered with metal particles (or clusters). After using MoCo@GW as a catalyst the amount of Mo and Co were decreased significantly but when MnO2 was added as a co-catalyst to solution, some particles of Co stayed on the glass wool.

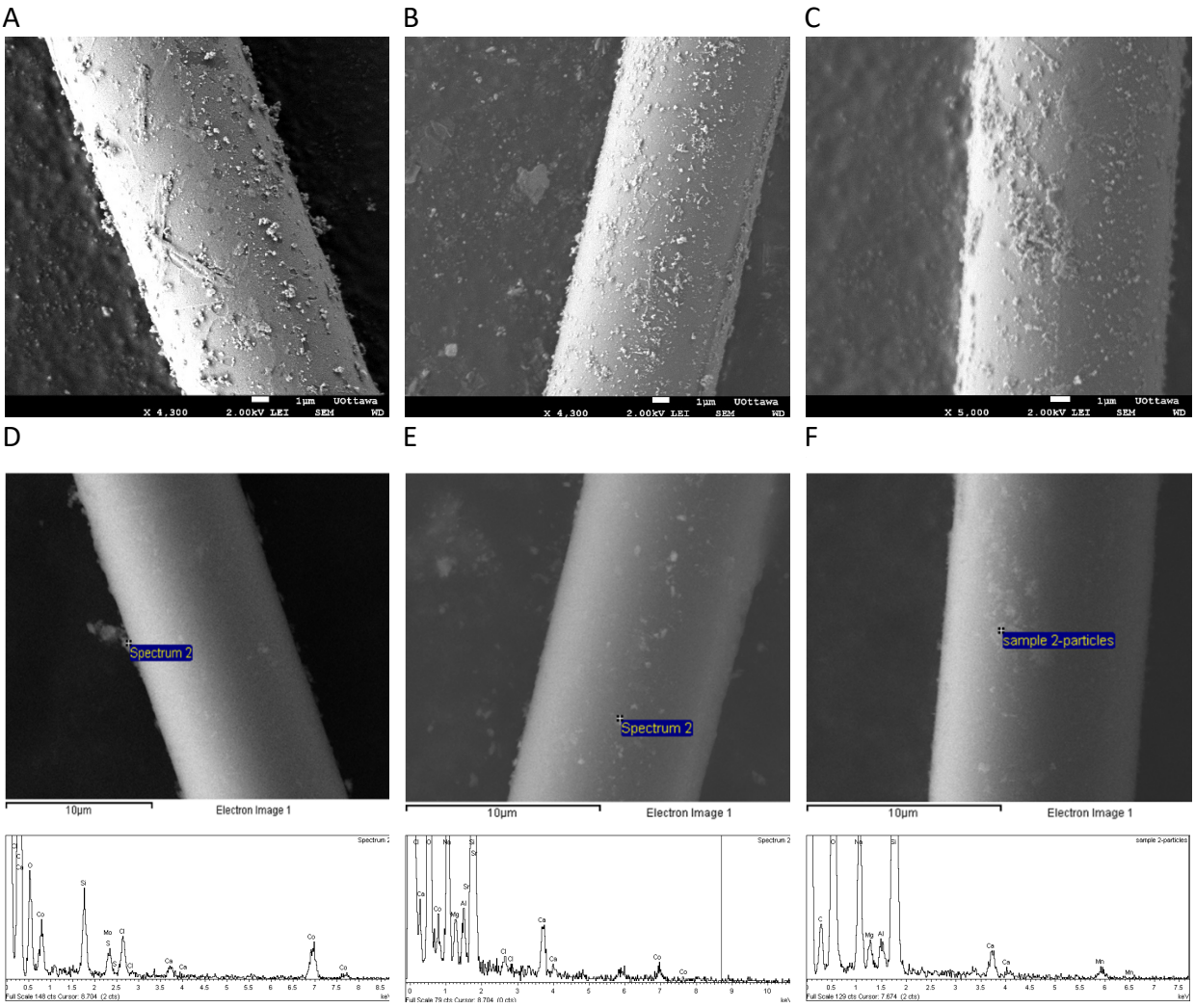

Figure S1. SEM images of catalysts

(A) fresh MoCo@GW, (B) used MoCo@GW in the presence of MnO2, and (C) fresh Mn@GW. EDX spectra for the corresponding region shown of (D) fresh MoCo@GW, (E) used MoCo@GW in the presence of MnO2, and (F) fresh Mn@GW. Scale bar = 1 μm. Fibers are about 10 μm in diameter.

XPS analysis

XPS deconvolution analyses were performed for MoCo@GW in order to determine the oxidation state of Mo and Co. Characteristic peaks for Mo 3d were proved MoS_2 and MoS_3 in our catalyst. These peaks were fitted using the spin-orbit split constituted by Mo^{4+} 3d5/2 (229.1 eV), Mo^{4+} 3d3/2 (232.1 eV), Mo^{6+} 3d5/2 (231.8 eV), and Mo^{6+} 3d3/2 (235 eV) separated by 3.2 eV. Peaks of $Mo^{\delta+}$ 3d5/2 (227.7 eV) and $Mo^{\delta+}$ 3d3/2 (230.7 eV) ($0 < \delta < 4$). Single peak at 226.6 eV were attributed to S^{2-} 2s that is overlapping part of Mo 3d peaks. S is from Mo precursor $(NH_4)_4MoS_4$ in MoCo@GW[3-5]

The XPS fitting for the Co 2p in MoCo@GW reveals the presence of two oxidation states. Co^{3+} 2p3/2 (779 eV) and Co^{3+} 2p1/2 (794 eV) separated by 14.99 eV and Co^{2+} 2p3/2 (781.2 eV) and Co^{2+} 2p1/2 (796.5 eV) followed by Co^{2+} 2p satellite peaks at (786 eV and 802.6 eV) is confirmation in presence of Co oxides.[6]

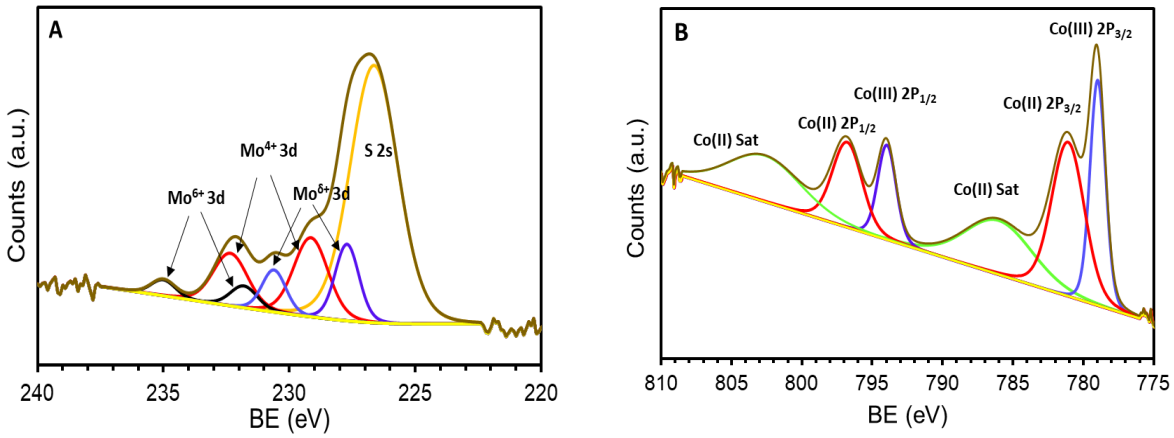

Figure S2. Deconvoluted HR-XPS spectrum of MoCo@GW (A) Mo 3d, (B) Co 2P

Photosensitized semi-oxidation of THIQ

This section provides conversion selectivity graphs for a variety of experimental conditions beyond those illustrated in graphs in the main text. These conditions supplement and provide additional support for the examples in the main text.

Reaction conditions

Typical experiments involve 67 mg of THIQ (0.125 M) in 4 mL of acetonitrile and visible light irradiation (LED: λmax = 450 nm, FWHM = 23 nm, irradiance ≤ 6 Wcm-2) under O_2 atmosphere. Air cooling system was used to maintain reaction temperature at about ~23 °C. A detailed spectroscopic analysis of this light source reveals a 0.02% content of light below 400 nm.

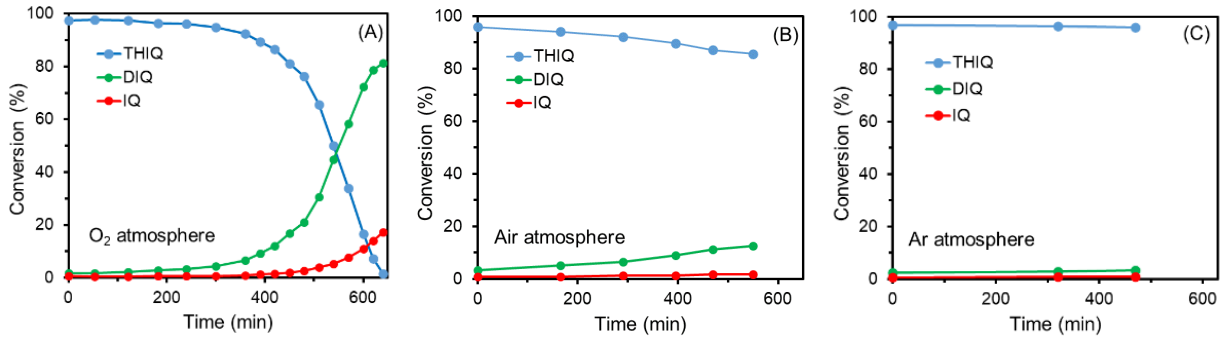

Figure S3. Effect of oxygen concentration
Semi-oxidation of THIQ (0.125 M) in AcN (in the absence of photosensitisers) irradiated with Blue LEDi under different atmospheres: (A) oxygen, (B) air, and (C) argon. Samples were analysed by GC-MS using tert-Butylbenzene as external standard.

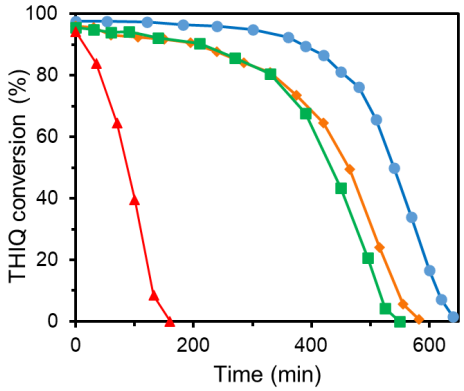

Figure S4. Effect of adding IQ and DHIQ in the oxidation of THIQ
THIQ (0.125 M) in 4 ml AcN, O_2 atmosphere, irradiated with Blue LEDi. Samples were analysed by GC-MS using tert-butylbenzene as an external standard. GC-MS results of experiments with different additives. In parenthesis, composition at time = 0.

(Blue circle) without added IQ. (THIQ 97.51%, DHIQ 1.82%, IQ 0.77%)
(Green square) with 4 %mol of commercial IQ (THIQ 95.45%, DHIQ 1.12%, IQ 3.43%)
(Orange diamond) with 4 %mol of commercial DHIQ (THIQ 95.94%, DHIQ 3.90%, IQ 0.16%)
(Red triangle) with 0.5ml of completed reaction IQ and DHIQ (THIQ 94.11%, DHIQ 4.18%, IQ 1.7%)

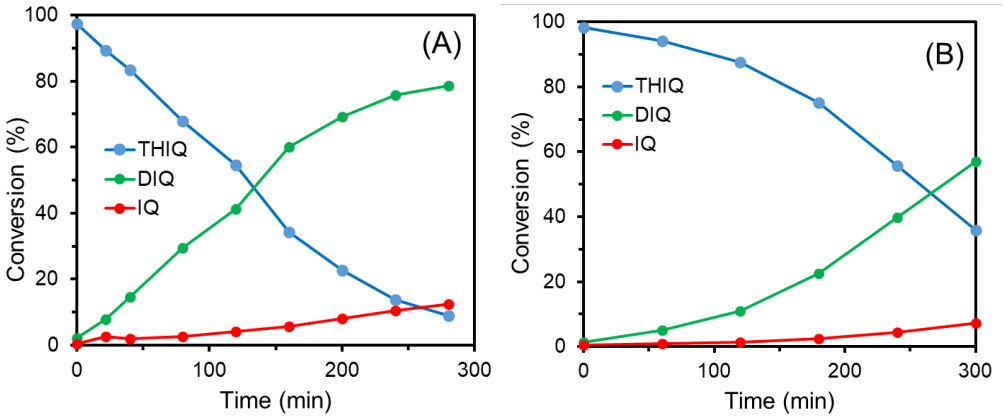

Figure S5. Effect of ruthenium-based sensitizers on the reaction progress
Semi-oxidation of THIQ (0.125 M) in AcN in the presence of a photosensitisers and irradiated with Blue LEDi under O_2 atmosphere: (A) $Ru(bpy)_3Cl_2$ (0.01mM) and (B) RuB@GW (50 mg). Samples were analysed by GC-MS using tert-Butylbenzene as external standard. Note that (A) is an homogeneous system, while (B) is heterogeneous.

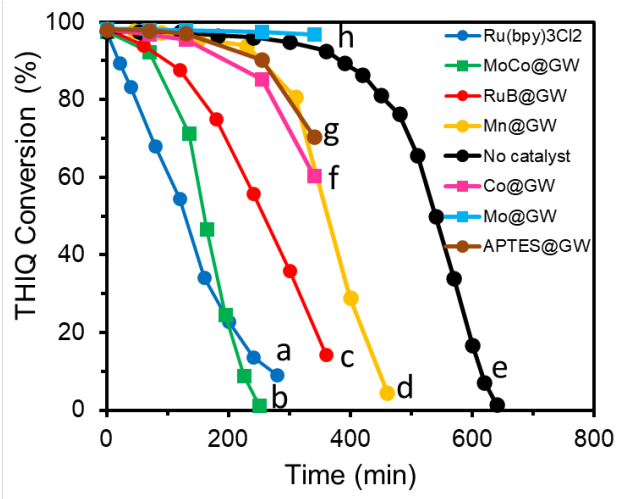

Figure S6. Comparison of different photosensitizers reported in this contribution with a few others that were tested in preliminary experiments.

Semi-oxidation of THIQ (0.125M) in AcN using different photosensitisers. All samples were irradiated with blue LEDi under O_2 atmosphere and analysed by GC-MS using tert-Butylbenzene as external standard. (a) $Ru(bpy)_2Cl_3$, (b)MoCo@GW, (c)RuB@GW, (d)Mn@GW, (e) no catalyst, (f) Co@GW, (g)APTES@GW, (h) Mo@GW.

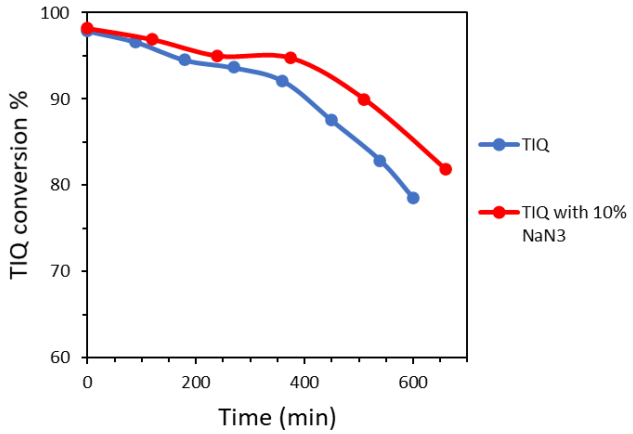

Figure S7. Effect of NaN_3 (a singlet oxygen scavenger) on catalyst performance
THIQ (0.125M) in methanol irradiated with blue LEDi (450 nm), samples were analysed with GC-MS. (blue) THIQ, (red) THIQ with 10 mol% NaN_3

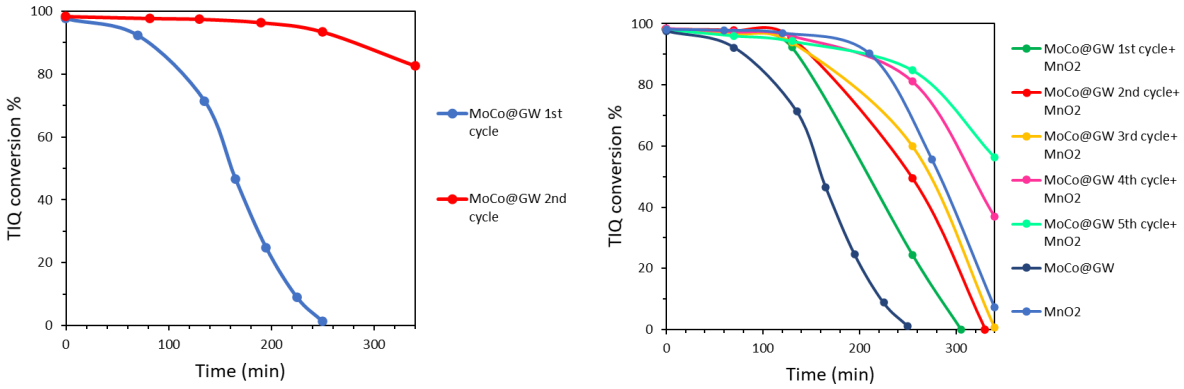

Figure S8. Effect of added MnO_2 on MoCo@GW performance and reusability.
All experiments were done with TIQ (0.125M) in AcN, oxygen atmosphere, irradiated with LEDi 450nm and samples analysed with GC-MS. (A) 2 cycles of MoCo@GW, (B) effect of adding MnO_2 as a co-catalyst to preserve MoCo@GW for next cycles.

References:

1. A. Elhage, B. Wang, N. Marina, M. L. Marin, M. Cruz, A. E. Lanterna and J. C. Scaiano, Glass wool: a novel support for heterogeneous catalysis, Chem. Sci., 2018, 9, 6844-6852.
2. R. I. Teixeira, N. C. de Lucas, S. J. Garden, A. E. Lanterna and J. C. Scaiano, Glass wool supported ruthenium complexes: versatile, recyclable heterogeneous photoredox catalysts, Cat. Sci. Tech., 2020, 10, 1273-1280.
3. A. V. Naumkin, A. Kraut-Vass, S. W. Gaarenstroom and C. J. Powell, in NIST Standard Reference Database 20, Version 4.1, 2012.
4. L. Zhang, L. Wu, J. Li and J. Lei, Electrodeposition of amorphous molybdenum sulfide thin film for electrochemical hydrogen evolution reaction, BMC Chemistry, 2019, 13, 88.
5. H. Wu and K. Lian, The Development of Pseudocapacitive Molybdenum Oxynitride Electrodes for Supercapacitors, ECS Transactions, 2014, 58.
6. M. Biesinger, B. Payne, A. Grosvenor, L. Lau, A. Gerson and R. Smart, Resolving surface chemical states in XPS analysis of first row transition metals, oxides and hydroxides: Cr, Mn, Fe, Co and Ni, Applied Surface Science, 2011, 257, 2717-2730.